JOURNAL of
MATERIALS and MECHATRONICS:A

e-ISSN 2717-8811
JournalMM, 2025, 6(2), 353-365
https://doi.org/10.55546/jmm.1717116

**Araştırma Makalesi / Research Article**

# In Vitro Evaluation of Pore Size and Weight Changes of Elderberry-Enriched Carboxymethyl Chitosan in Various Biological Fluids

Bilge Cansu UZUN SAYLAN[1*], Gizem Baysan[2], Osman YILMAZ[3], Safiye AKTAŞ[4], Hasan HAVİTCİOGLU[2,5]

[1*] Dokuz Eylul University, Faculty of Dentistry, Department of Periodontology, Izmir, Türkiye,
ORCID ID: https://orcid.org/0000-0002-4896-3864, bilgecansu.uzunsaylan@deu.edu.tr
[2] Dokuz Eylul University, Institute of Health Science, Department of Biomechanics, Izmir, Türkiye,
ORCID ID: https://orcid.org/0000-0002-3195-9156, gizemciner@gmail.com
[3] Dokuz Eylul University, Faculty of Medicine Experimental Animals Laboratory, Izmir, Türkiye,
ORCID ID: https://orcid.org/0000-0001-7817-7576, osman.yilmaz@deu.edu.tr
[4] Dokuz Eylul University, Institute of Oncology, Department of Basic Oncology, Izmir, Türkiye,
ORCID ID: https://orcid.org/0000-0002-7658-5565, safiyeaktas@gmail.com
[5] Dokuz Eylul University, Faculty of Medicine, Department of Orthopedics and Traumatology, Izmir Türkiye,
ORCID ID: https://orcid.org/0000-0001-8169-3539, hhvtci@gmail.com

**Geliş/ Received:** 11.06.2025**;** **Revize/Revised:** 10.09.2025 **Kabul / Accepted:** 09.11.2025

**ABSTRACT:** The interaction between biomaterials and biological fluids plays a critical role in determining the swelling behavior, biodegradation profile, and integration capacity of scaffolds used in periodontal and peri-implant tissue engineering. This study aimed to analyze the pore structure and weight changes of an elderberry (*Sambucus nigra*) extract-enriched carboxymethyl chitosan (CMCht-E) biomaterial following exposure to various biological fluids, including normal saline, serum, heparinized blood, and saliva. CMCht-E biomaterial discs were incubated for 24 and 72 hours in normal saline, rat serum, heparinized blood, and saliva. Fluid–biomaterial interactions were evaluated based on microscopic pore diameter measurements and changes in sample weight. Data were statistically analyzed using one-way ANOVA and paired t-tests ($p<0.05$). Initial weights and pore diameters were comparable among all groups ($p>0.05$). At 72 hours, the greatest weight gain was observed in the saliva group, whereas the largest pore diameter was recorded in the blood group ($p<0.001$). Changes in pore diameter were minimal in the normal saline group. Microscopic analyses revealed pore coalescence and enlargement, particularly in blood and saliva environments. The CMCht-E biomaterial exhibited structure- and volume-responsive behavior depending on the characteristics of the biological fluid it interacted with. These findings support its potential for functional optimization based on the target application, reinforcing its clinical relevance in terms of controlled degradation, cellular infiltration, and tissue integration.

**Keywords:** Carboxymethyl chitosan, Elderberry, Pore diameter, Biological fluids

*Sorumlu yazar / Corresponding author: bilgecansu.uzunsaylan@deu.edu.tr
Bu makaleye atıf yapmak için /To cite this article

Uzun Saylan, B. C., Baysan, G., Yılmaz, O., Aktaş, S., Havitcioglu, H. (2025). In Vitro Evaluation of Pore Size and Weight Changes of Elderberry-Enriched Carboxymethyl Chitosan in Various Biological Fluids. Journal of Materials and Mechatronics: A (JournalMM), 6(2), 353-365.

## 1. INTRODUCTION

Periodontitis is a chronic inflammatory disease with a multifactorial etiology, characterized by an imbalance in the host–microbial interaction in favor of the host response. It involves intense inflammatory cell infiltration, destruction of connective tissue, formation of periodontal pockets, and resorption of alveolar bone (Meyle & Chapple, 2015). The global prevalence of periodontal disease ranges between 20% and 50% (Sanz, 2010). As one of the leading causes of tooth loss, periodontitis adversely affects mastication, esthetics, self-confidence, and overall quality of life (Reynolds & Duane, 2018). With the increased use of dental implants due to tooth loss, peri-implant diseases have become a major clinical concern. Peri-implantitis shares pathogenic mechanisms with periodontitis and is further influenced by microbial colonization, biomechanical stress, host immune response, and systemic conditions (Schwarz et al., 2018). It has been reported that approximately 80% of patients develop peri-implant mucositis and 28–56% develop peri-implantitis within 5 to 10 years after implant placement (Yu et al., 2024). Therefore, the development of effective, biocompatible, and clinically applicable approaches for the prevention and treatment of periodontal and peri-implant diseases has become a priority in contemporary research (Larsson et al., 2016).

Recent advancements in biomaterials science and tissue engineering have enabled the design of biomimetic scaffold systems for the regeneration of periodontal and peri-implant tissues (Brouwer et al., 2015). Regenerative strategies and biomaterial-based therapies have emerged as effective methods for restoring the integrity of both hard and soft tissues surrounding teeth and implants. Consequently, the development of novel biomaterials with biocompatible, biodegradable, and antimicrobial properties holds significant clinical relevance (Zhang et al., 2024).

Tissue engineering is a multidisciplinary approach that combines cells, biomaterials, and biochemical factors to restore or replace damaged tissues. In the regeneration of periodontal and peri-implant tissues, scaffold materials play a critical role in supporting cellular proliferation, differentiation, and tissue integration (Bharadwaz & Jayasuriya, 2020). For these biomaterials to be effective, they must exhibit appropriate pore architecture and controlled degradability to facilitate intercellular communication and tissue remodeling (Kim et al., 2014). Such materials provide a favorable microenvironment for both hard and soft tissue regeneration and are considered fundamental components in tissue engineering applications (Zhao et al., 2019a).

Chitosan is a naturally abundant biopolymer, and its derivative, carboxymethyl chitosan (CMCht), is a water-soluble form with enhanced compatibility in biological systems (Kumar et al., 2019). Due to its antimicrobial, antioxidant, and hemostatic properties, CMCht is widely utilized in wound healing and regenerative medicine (Zhao et al., 2019b). In recent years, incorporating naturally derived phenolic compounds into biomaterial structures has been shown to enhance their biological activity (Kumar et al., 2019). Sambucus nigra (elderberry), known for its strong antioxidant capacity as well as anti-inflammatory and antimicrobial properties, has been evaluated as a bioactive additive to improve the functionality of biomaterials (Haș et al., 2023).

Pore structure is a critical parameter in the regenerative potential of biomaterials, as it directly affects cellular migration, tissue vascularization, extracellular matrix remodeling, and overall integration with host tissue (Bharadwaz & Jayasuriya, 2020). Thus, the porosity of a biomaterial plays a decisive role in creating a suitable microenvironment for cellular viability and tissue integration; (Venkatesan & Kim, 2014) however, increased porosity may be associated with a reduction in mechanical strength. Therefore, when designing an effective porous structure, both the physical and the chemical/biological properties of the material should be carefully considered(Maksoud et al., 2022). Structural changes in pore diameter over time, when exposed to different biological fluids,

provide valuable insight into the material's swelling behavior, mechanical stability, and adaptability to the biological environment (Haș et al., 2023; Kumari et al., 2022).

This study aims to investigate the in vitro weight changes and microscopic pore diameter alterations of elderberry-enriched carboxymethyl chitosan (CMCht-E) biomaterial following 24- and 72-hour incubations in different biological fluids including normal saline, serum, blood, and saliva, as our comprehensive in vitro research previously demonstrated that CMCht-E exhibited superior antibacterial, antioxidant, and regenerative properties compared to CMCht(Baysan et al., 2024), and was therefore considered the most promising candidate for future clinical applications.

## 2. MATERIALS AND METHODS

This study was conducted in the Experimental Animal Laboratory with the approval of the Dokuz Eylul University Local Ethics Committee for Animal Research (Protocol No: 44/2023).

### 2.1 Preparation of CMCht-E Biomaterial

The CMCht-E biomaterial was prepared by dissolving 2.5% (w/v) O-carboxymethylated chitosan (CMCht; Santa Cruz Biotechnology, Cat. No: 358091) in distilled water containing elderberry extract at a concentration of 0.05 mg/mL (w/v). The elderberry extract was a commercially available powdered product (NatureHerb Store, China), obtained through 100% ethanol extraction. The mixture was stirred with a magnetic stirrer for approximately 2 hours to ensure homogeneity. For every 5 mL of solution, 0.04 g of PEGDE (Sigma-Aldrich, Mn = 500, 475696) was added as a crosslinking agent. The mixture was then incubated at 40°C in a vacuum oven for 48 hours to allow hydrogel formation. Following gelation, the samples were frozen at –20°C for 12 hours, then lyophilized at –25°C under 0.1 mbar pressure for 48 hours to obtain a sponge-like scaffold structure(Baysan et al., 2024). The completely dried hydrogel scaffolds were punched into discs of 5 mm diameter and 2 mm thickness using a biopsy punch, sterilized in ethylene oxide, and prepared for experimental application.

### 2.2 Preparation of Biological Fluids

One female Wistar Albino rat weighing 250–300 grams was used in the study. Following anesthesia, a V-shaped abdominal incision was performed to expose the posterior vena cava, and venous blood was collected using a 21G needle. The rat was sacrificed due to hypovolemic shock during the procedure. Of the 10 mL of blood collected, 5 mL was centrifuged at 3000 rpm for 5 minutes to isolate serum, while the remaining 5 mL was mixed with heparin to obtain a heparinized whole blood sample. Additionally, for this in vitro study, approximately 10 mL of saliva was collected from a systemically healthy, non-smoking adult volunteer into a sterile tube (Sindhusha & Doraiswamy, 2023).

### 2.3 LSTM (Long short-term memory)

Sample size was predetermined using G*Power 3.1.9.7 (Cohen's $d = 0.8$, $\alpha = 0.05$, power = 0.95), which indicated a minimum of 7 specimens per group. Prepared CMCht-E scaffolds were divided into four groups (n=14 per fluid group), and their dry weights were measured using a precision balance. The samples were incubated in four different media: normal saline (NS), serum, heparinized whole blood, and saliva. All groups were incubated at 37°C for 24 and 72 hours.

### 2.4 Evaluation Methods

Weighing: After 24 and 72 hours of incubation in normal saline, blood, and serum, seven samples from each group were removed, and surface fluids were gently blotted with filter paper. The

samples were then weighed using a precision balance **(**Mettler Toledo AB204-S**).** The fluid absorption was calculated based on the initial dry weight of each sample and compared across groups.

Microscopic evaluation: Paraffin-embedded sections obtained from the dry control group and the samples incubated in normal saline, serum, blood, and saliva were examined under a light microscope **(**Olympus BX51). From both the 24-hour and 72-hour timepoints, 5-µm-thick sections were assessed under 400× magnification using a direct view camera **(**Olympus SC50) without staining. The number and diameter of vacuoles were evaluated using an image analysis system **(**CellSens, Olympus, Tokyo, Japan). To ensure standardization, one representative pore diameter was identified and marked in each material sample, as illustrated in Figure 1, and these measurements were used to calculate the mean pore diameters. The resulting data were utilized to compare microstructural changes in pore architecture among groups.

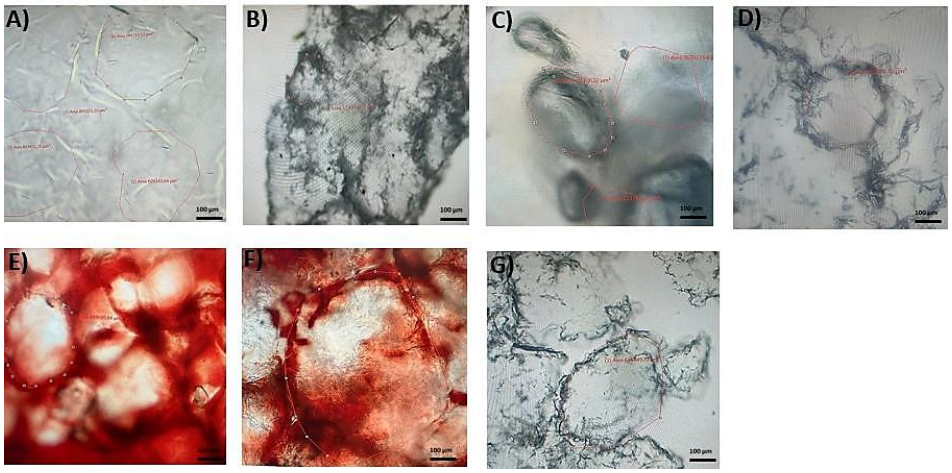


**Figure 1.** Pore areas are outlined in red in the images. A) NS – 24 h; B) NS – 72 h; C) Serum – 24 h; D) Serum – 72 h; E) Blood – 24 h; F) Blood – 72 h; G) Saliva – 72 h. (Magnification: ×400; measurement unit: µm²)

### 2.5 Statistical Analysis

All statistical analyses were performed using SPSS version 22.0. Descriptive statistics were presented as number and percentage for categorical variables, and as mean ± standard deviation for numerical variables. The Kolmogorov–Smirnov test was used to assess the normality of data distribution. For comparing three or more independent groups, one-way ANOVA was used when the data showed normal distribution; otherwise, the Kruskal–Wallis test was applied. For paired group comparisons, the paired t-test was used under normal distribution conditions; otherwise, the Wilcoxon signed-rank test was employed. A p-value $< 0.05$ was considered statistically significant.

## 3. RESULTS AND DISCUSSION

### 3.1 Results

#### 3.1.1 Pore Diameter Changes in Different Biological Fluids

The pore diameter of the biomaterial was measured after 24 and 72 hours of incubation in normal saline (Figure 2A), serum (Figure 2B), heparinized blood (Figure 2C), and saliva (Figure 2D), and the mean pore diameters were compared across groups (Table 1).

Following incubation of the CMCht-E biomaterial in various biological fluids, statistically significant changes in pore diameter were observed (Figure 3). Initially, the pore diameter of the dry biomaterial was similar across all groups, with no significant differences detected ($p = 1.000$).

However, after 24 hours, the largest pore diameter was recorded in the saliva group (764,499.1 ± 999,969.5 µm²), while the smallest was observed in the normal saline group (9,237.9 ± 1,920.7 µm²). This trend persisted at 72 hours, with a significant increase in pore diameter in the blood group, reaching the highest value (2,346,447.3 ± 369,306.2 µm²) ($p < 0.001$). The increase in the normal saline group remained relatively limited compared to the other fluids (125,651.2 ± 49,200.7 µm²). Statistical analyses demonstrated that the differences in pore diameter were significantly influenced by both the type of fluid and the incubation duration ($p < 0.001$, Repeated Measures ANOVA).

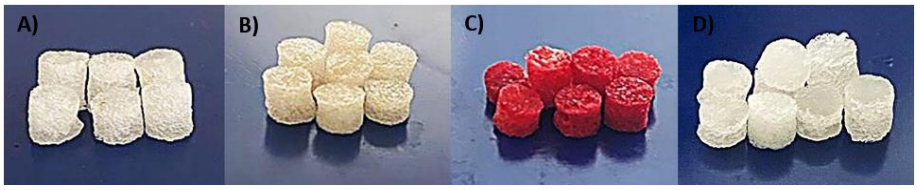


**Figure 2.** Representative appearance of the biomaterial after 72 hours of incubation in different biological fluids: A) Normal saline, B) Serum, C) Blood, D) Saliva

**Table 1.** Mean Pore Area of CMCht-E Biomaterial in Different Biological Fluids

| Fluids | Dry Biomaterial (µm²) | 24 h (µm²) | 72 h (µm²) | p-value | Post Hoc |
|---|---|---|---|---|---|
| **Normal saline (NS)** | 218,312.9 ± 70,369.0 | 9,237.9 ± 1,920.7 | 125,651.2 ± 49,200.7 | <0.001** | 1–2, 2–3 |
| **Serum** | 218,411.3 ± 71,360.0 | 373,963.4 ± 87,710.1 | 325,422.3 ± 56,947.7 | 0.015** | 1–2, 1–3 |
| **Blood** | 217,419.7 ± 71,692.0 | 595,849.2 ± 263,626.1 | 2,346,447.3 ± 369,306.2 | <0.001** | 1–2, 1–3, 2–3 |
| **Saliva** | 219,578.8 ± 72,471.0 | 764,499.1 ± 999,969.5 | 554,140.4 ± 109,821.9 | <0.001** | 1–2, 1–3, 2–3 |
| p-value | 1.000* | <0.001* | <0.001* | | |

1- Dry biomaterial, 2- 24 h, 3-72 h
*One-way ANOVA, **Repeated Measures ANOVA

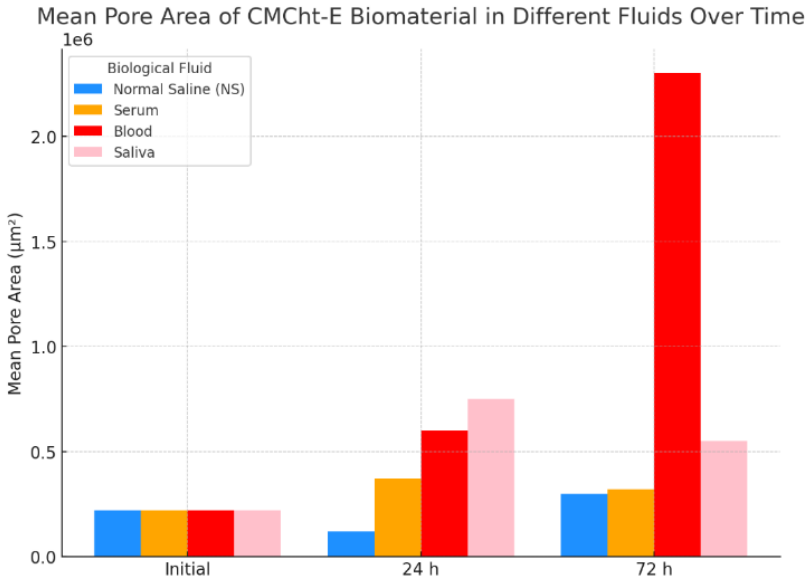


**Figure 3.** Bar chart showing changes in the mean pore area (µm²) of CMCht-E biomaterial after incubation in different biological fluids at three time points: initial (dry), 24 hours, and 72 hours. Each time point includes four bars representing incubation in: Normal Saline (NS) (yellow), Serum (orange), Blood (red), and Saliva (pink)

### 3.1.2 Weight Change in Different Fluids

To evaluate the fluid absorption capacity of the biomaterial in different liquid environments, weight measurements were conducted at baseline, 24 hours, and 72 hours of incubation (Table 2). No statistically significant differences were observed among the initial weights of the groups ($p = 1.000$). After 24 hours, the highest increase in weight was observed in the saliva group (317.8 ± 1.2 mg), followed by blood (308.2 ± 0.5 mg), normal saline (266.2 ± 0.9 mg), and serum (252.6 ± 0.1 mg). At 72 hours, the highest weight was again recorded in the saliva group (364.5 ± 0.5 mg), while the lowest was found in the serum group (281.3 ± 2.3 mg) (Figure 4). Weight gain was found to be statistically significant depending on both incubation time and the type of biological fluid ($p < 0.001$, Repeated Measures ANOVA and Kruskal–Wallis tests).

The appearance of the biomaterial after 24 hours of incubation in different fluids is shown in Figure 5, while the images after 72 hours are presented in Figure 6.

**Table 2.** Weight Change of CMCht-E Biomaterial in NS, Serum, Blood, and Saliva

| **Fluids** | **Initial (mg)** | **24 h (mg)** | **72 h (mg)** | p-value | Post Hoc |
|---|---|---|---|---|---|
| **Normal saline (NS)** | 21.7 ± 0.01 | 266.2 ± 0.9 | 360.9 ± 0.6 | <0.001¥ | 1–2, 1–3, 2–3 |
| **Serum** | 21.5 ± 0.9 | 252.6 ± 0.1 | 281.3 ± 2.3 | <0.001ǂ | 1–2, 1–3 |
| **Blood** | 21.7 ± 0.04 | 308.2 ± 0.5 | 291.6 ± 0.9 | <0.001ǂ | 1–2, 1–3, 2–3 |
| **Saliva** | 21.6 ± 0.35 | 317.8 ± 1.2 | 364.5 ± 0.5 | <0.001ǂ | 1–2, 1–3, 2–3 |
| p-value | 1.000* | <0.001* | <0.001** | | |

1- Dry biomaterial, 2- 24 h, 3-72 h

*One-way ANOVA, **Kruskal–Wallis, ǂ Repeated Measures ANOVA, ¥ Friedman Test

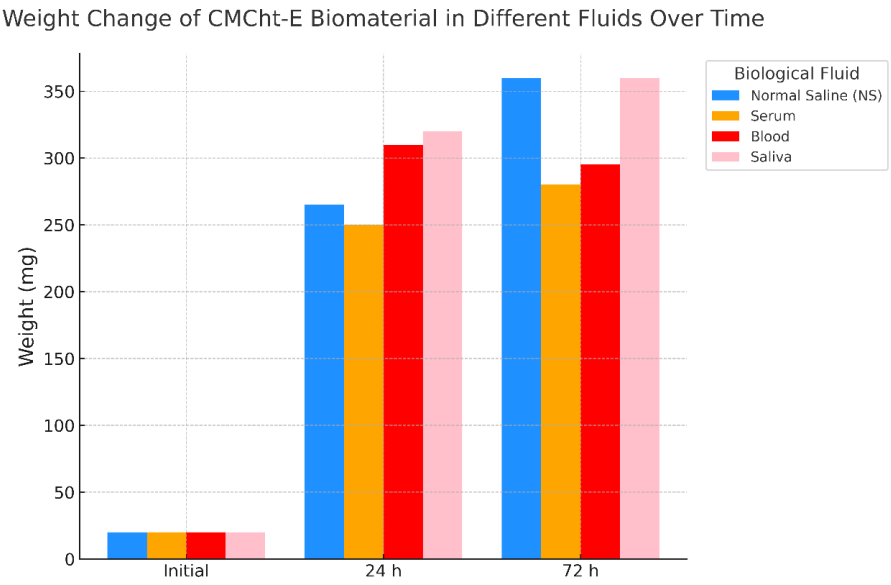


**Figure 4.** Bar chart illustrating the weight change (mg) of CMCht-E biomaterial after incubation in different biological fluids at three time points: initial (dry), 24 hours, and 72 hours. Each time point includes four bars representing incubation in: Normal Saline (NS) (yellow), Serum (orange), Blood (red), and Saliva (pink)

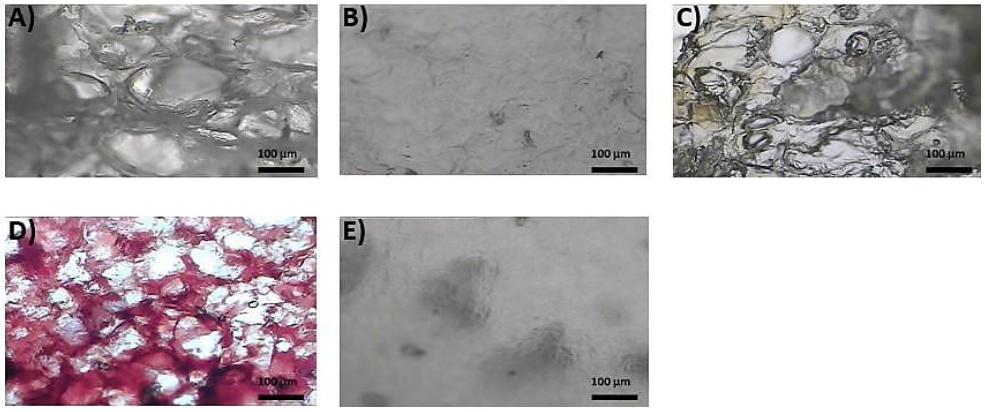


**Figure 5.** A) Dry biomaterial; B) NS – 24 h; C) Serum – 24 h; D) Blood – 24 h; E) Saliva – 24 h. (Magnification: ×400; measurement unit: µm²)

As a result of the analysis of the test results, no significant performance difference was found between the ADAM and SGD optimization algorithms. At the same time, the SGD algorithm resulted in longer training times. Therefore, in order to minimize the computational cost, the studies were continued with the ADAM optimization algorithm.

### 3.2 Discussion

In tissue engineering, the primary goal is to ensure that the scaffold temporarily implanted in damaged or compromised tissue sites not only supports regeneration but also gradually degrades to allow the replacement of newly formed tissue (Kievit et al., 2010). Three-dimensional scaffolds made from synthetic or biopolymeric materials should support cell migration and proliferation, allowing the reconstruction of tissues with the desired structure and function at the target site (Dec et al., 2022). Carboxymethylated chitosan, a biopolymer derivative, possesses extensive potential for biomedical applications (Shariatinia, 2018). Compared to chitosan, carboxymethyl chitosan (CMCht-E) offers improved solubility and processability for tissue engineering applications, and it facilitates enhanced cell adhesion and proliferation (Van der Schueren et al., 2012). In addition to its biocompatibility, its porous structure enables the incorporation of drugs or bioactive molecules, and its biodegradability allows for the controlled release of these agents (Kruczkowska et al., 2024).

The degradability of tissue engineering scaffolds is a critical parameter for their success. This enhanced degradation behavior may be attributed to the scaffold's hydrophilic nature. In a successful tissue engineering application, the implanted scaffold should gradually be replaced by native tissues over time, a process that relies entirely on the scaffold's biodegradability (Unnithan et al., 2016).

The swelling behavior of scaffolds is another crucial parameter to be evaluated. It significantly influences cell adhesion, growth, and proliferation (Sivashankari & Prabaharan, 2020). The swelling ratio indicates the scaffold's fluid absorption capacity. Cells embedded within the scaffold draw nutrients from the absorbed fluid; however, excessive swelling can increase pore size and negatively affect cell adhesion and proliferation. Therefore, a controlled swelling capacity is desired. A scaffold with a low swelling ratio provides a more stable environment for cell survival, contributing to successful tissue formation and scaffold performance (Unnithan et al., 2016).

Given the increasing use of polymeric materials designed for specific biological environments, modern drug delivery systems are becoming more prevalent in biomedical applications. Biopolymers, in particular, play a vital role in controlled drug delivery due to their renewability, non-toxicity, low cost, biodegradability, and excellent biological performance (Pooresmaeil & Namazi, 2021; Behzadi Nia et al., 2020).

This study evaluated the pore size and swelling behavior of carboxymethyl chitosan (CMCht-E) based biomaterial in serum, heparinized blood, and normal saline (NS) environments. The findings indicate that the biomaterial undergoes significant structural changes depending on the type of biological fluid and duration of incubation. These variations are believed to result from interactions between the biomaterial and the proteins, ions, and cellular components present in the fluids.

NS exhibited the lowest pore size values at 24 hours, suggesting that this isotonic environment had a limited effect on the pore structure, keeping it relatively compact. At 72 hours, weight gain became more evident; however, this increase did not correspond proportionally to pore expansion. This may be explained by NS promoting water-based swelling, initially affecting the peripheral pores of the material and then gradually extending throughout the scaffold. The low protein content in NS may have initially restricted matrix swelling, but as ionic diffusion progressed, a modest increase in swelling was observed. This observation aligns with literature indicating that CMCht-E structures exhibit swelling behavior depending on the ionic strength of their environment (Spinks et al., 2006).

In the serum group, a significant increase in pore diameter was detected at both 24 and 72 hours. This may be attributed to the diffusion of proteins (e.g., albumin) and ions into the biomaterial matrix, causing pore expansion. Additionally, their pH responsiveness and swelling properties support their use in controlled drug delivery (Bao et al., 2014; Gao et al., 2019). The serum group exhibited a more controlled swelling profile, with moderate increases in weight and pore size compared to the other fluids, suggesting that serum induces a more predictable and stable response in the biomaterial. The differences observed among the biological fluids may also be partly explained by their pH levels, which influence the ionization of carboxyl and amino groups within the CMCht matrix. Normal saline (0.9% NaCl, pH ~5.5) has a slightly acidic character(Reddi, 2013), which may have limited the ionization process and contributed to the restricted swelling and more stable pore profile observed in this group. Saliva (pH ~6.2–7.6)(Bechir et al., 2021), although closer to neutral, exhibited more pronounced pore enlargement and swelling behavior, particularly at 24 hours, likely due to its protein and enzyme content. Serum and blood, with slightly alkaline pH values (~7.3–7.4)(Kellum, 2000), promoted stronger ionic interactions, resulting in a controlled increase in serum and a dramatic pore enlargement in blood at 72 hours. The sensitivity of carboxymethyl chitosan to environmental pH has been reported in previous studies, where changes in ionization states directly affected its fluid absorption and microstructural properties (Bao et al., 2014; Li et al., 2019). Thus, the pH-related responsiveness of CMCht-E likely contributes to the variations in pore diameter and weight gain observed across the different media.

In whole blood, a more complex response pattern was observed. Although pore diameters continued to increase up to 72 h, the weight reached an earlier peak and subsequently declined between 24 and 72 h. This paradoxical behavior can be associated with platelet-mediated clot retraction, which progressively compacts the fibrin mesh and expels entrapped fluid, thereby reducing overall weight despite ongoing structural expansion (Lam et al., 2011; Tutwiler et al., 2016). In addition, proteolytic activity and enzymatic degradation within the blood environment may have contributed to the relaxation of the hydrogel network, which could explain the sustained pore enlargement despite reduced fluid retention (Dash et al., 2011). The colloidal nature of blood and cellular interactions may also play a role, as red blood cell and platelet adhesion to the scaffold surface followed by lysis has been reported to influence initial swelling and subsequent weight changes (Weber et al., 2018). Similar observations have highlighted the hemostatic and swelling behavior of CMCht-based hydrogels in contact with blood, further supporting the present findings (Fakhr et al., 2020).This dual mechanism highlights the dynamic interplay between clot physiology and

biomaterial responsiveness, underscoring the unique challenges of evaluating hydrogels in direct contact with whole blood. Compared to the other biological fluids, serum and whole blood showed lower weight gain despite evident pore enlargement. In serum, this can be explained by ionic and protein interactions stabilizing fluid uptake, whereas in whole blood, platelet-driven clot retraction and proteolytic activity likely reduced fluid retention while allowing pore expansion.

In the saliva group, increases in both pore diameter and weight were more prominent compared to other fluids. This suggests that the protein and enzyme content of saliva provides an environment that facilitates interaction and diffusion into the biomaterial matrix (Marsh et al., 2016). Among all tested fluids, saliva induced the most dramatic response in terms of weight gain, reaching nearly six-fold absorption at 72 h, making it the biological fluid with the greatest swelling capacity. Concomitant pore enlargement was also detected, suggesting that salivary proteins and enzymes strongly influence scaffold microstructure. Previous studies have highlighted the sensitivity of chitosan-based scaffolds to protein- and enzyme-rich oral environments (Feng et al., 2024; Ryu et al., 2020), while the effects of pH and ionic strength on CMCht swelling have also been reported (Jaikumar et al., 2015; Lin et al., 2023). Our findings extend these observations by providing the first quantitative assessment of swelling in carboxymethyl chitosan scaffolds in human saliva. Although recent investigations have examined scaffold performance in saliva—reporting parameters such as porosity and surface morphology (Sindhusha & Doraiswamy, 2023) these evaluations were limited to single-timepoint or morphology-based assessments, without directly quantifying swelling kinetics. In contrast, our study provides the first time-resolved, quantitative evidence of pronounced swelling in CMCht-E scaffolds, documenting both weight gain and concomitant pore enlargement, and demonstrating a marked increase from 24 to 72 h. This dual effect has important implications: on one hand, it may facilitate drug diffusion and controlled release, supporting applications in oral and periodontal tissue engineering; on the other hand, excessive swelling could compromise scaffold stability under physiological conditions, underscoring the need for optimized crosslinking strategies. While these results are promising, it should also be acknowledged that saliva was collected from a single healthy volunteer. Considering the interindividual variability in salivary proteins, enzymes, and ionic content, future studies involving multiple participants are warranted to strengthen the generalizability of these findings.

This study demonstrated that the interaction of CMCht-E with different biological fluids results in significant structural modifications, supporting its potential for biomedical applications. Its high fluid absorption, adaptability to environmental conditions, and porous structural transformation make it a promising candidate for tissue engineering scaffolds. However, maintaining these changes within controlled limits is critical for ensuring mechanical stability and tissue integration. Future studies should explore scaffold modifications using different crosslinkers, in vivo biocompatibility assessments, and antimicrobial efficacy testing.

## 4. CONCLUSIONS

Structural analyses revealed that the CMCht-E biomaterial undergoes fluid-specific morphological modifications, including significant swelling and pore enlargement in saliva and blood. These findings confirm its responsiveness to complex biological environments and underscore its translational potential. Such dynamic behavior suggests that CMCht-E scaffolds can be applied not only in regenerative dentistry and maxillofacial tissue engineering but also as platforms for controlled drug delivery. While the results demonstrate promising structural adaptability, further

investigations using larger sample sizes, diverse biological fluids, and clinically relevant in vivo models are warranted to optimize crosslinking strategies, ensure long-term stability, and validate clinical applicability.

## 5. ACKNOWLEDGEMENTS

We thank Dr. Serdar Karakullukçu, M.D. for his assistance with statistical analysis and valuable comments.

## 6. CONFLICT OF INTEREST

Authors approve that to the best of their knowledge, there is not any conflict of interest or common interest with an institution/organization or a person that may affect the review process of the paper.

## 7. AUTHOR CONTRIBUTION

Bilge Cansu UZUN SAYLAN contributed to the management of the concept and/or design process of the research, data collection, preparation of the manuscript, final approval and full responsibility. Gizem BAYSAN contributed to the determining the concept and/or design process of the reseach, preparation of the manuscript, final approval and full responsibility. Osman YILMAZ contributed to the determining the concept and/or design process of the reseach, preparation of the manuscript, management of the concept and/or design process of the research, data collection, preparation of the manuscript, final approval and full responsibility. Safiye AKTAŞ contributed to the data analysis and interpretation of the results, critical analysis of the intellectual content, final approval and full responsibility. Hasan HAVİTÇİOĞLU contributed to the determining the concept and/or design process of the reseach, critical analysis of the intellectual content, final approval and full responsibility.

## 8. REFERENCES

Bao D., Chen M., Wang H., Wang J., Liu C., Sun R., Preparation and characterization of double crosslinked hydrogel films from carboxymethylchitosan and carboxymethylcellulose. Carbohydrate Polymers 110, 113–120, 2014.

Baysan G., Yilmaz P.A., Husemoglu R.B., Albayrak A.Z., Sisman A.R., Havitcioglu H., Elderberry (Sambucus nigra) and hawthorn (Crataegus oxyacantha) extract additives in carboxymethyl chitosan scaffolds for osteochondral tissue engineering applications. Journal of Applied Polymer Science 141(28), 2024.

Bechir, F., Pacurar, M., Tohati, A., & Bataga, S. M. Comparative Study of Salivary pH, Buffer Capacity, and Flow in Patients with and without Gastroesophageal Reflux Disease. International Journal of Environmental Research and Public Health 19(1), 2021.

Behzadi Nia S., Pooresmaeil M., Namazi H., Carboxymethylcellulose/layered double hydroxides bio-nanocomposite hydrogel: A controlled amoxicillin nanocarrier for colonic bacterial infections treatment. International Journal of Biological Macromolecules 155, 1401–1409, 2020.

Bharadwaz A., Jayasuriya A.C., Recent trends in the application of widely used natural and synthetic polymer nanocomposites in bone tissue regeneration. Materials Science and Engineering: C 110, 110698, 2020.

Brouwer K. M., Lundvig D. M. S., Middelkoop E., Wagener F. A. D. T. G., Von den Hoff J. W., Mechanical cues in orofacial tissue engineering and regenerative medicine. Wound Repair and Regeneration 23(3), 302–311, 2015.

Dash M., Chiellini F., Ottenbrite R. M., Chiellini, E., Chitosan—A versatile semi-synthetic polymer in biomedical applications. Progress in Polymer Science 36(8), 981–1014, 2011.

Dec P., Modrzejewski A., Pawlik A., Existing and novel biomaterials for bone tissue engineering. International Journal of Molecular Sciences 24(1), 529, 2022.

Fakhri E., Eslami H., Maroufi P., Pakdel F., Taghizadeh S., Ganbarov K., Yousefi M., Tanomand A., Yousefi B., Mahmoudi S., Kafil, H. S., Chitosan biomaterials application in dentistry. International Journal of Biological Macromolecules 162, 956-974, 2020.

Feng M., Zeng X., Lin Q., Wang Y., Wei H., Yang S., Wang G., Chen X., Guo M., Yang X., Hu J., Zhang Y., Yang X., Du Y., Zhao Y., Characterization of Chitosan-Gallic Acid Graft Copolymer for Periodontal Dressing Hydrogel Application. Advanced Healthcare Materials 13(7), 2024.

Gao J., Xu Y., Zheng Y., Wang X., Li S., Yan G., Wang J., Tang R., pH-sensitive carboxymethyl chitosan hydrogels via acid-labile ortho ester linkage as an implantable drug delivery system, Carbohydrate Polymers 225, 115237, 2019.

Haș I. M., Teleky B. E., Szabo K., Simon E., Ranga F., Diaconeasa Z. M., Purza A. L., Vodnar D. C., Tit D. M., Nițescu M., Bioactive potential of elderberry (Sambucus nigra L.): Antioxidant, antimicrobial activity, bioaccessibility and prebiotic potential, Molecules 28(7), 3099, 2023.

Jaikumar D., Sajesh K. M., Soumya S., Nimal T. R., Chennazhi K. P., Nair S. V., Jayakumar R. Injectable alginate-O-carboxymethyl chitosan/nano fibrin composite hydrogels for adipose tissue engineering. International Journal of Biological Macromolecules 74, 318–326, 2015.

Kellum J. A., Determinants of blood pH in health and disease. Critical Care 4(1), 6-14, 2000.

Kievit F. M., Florczyk S. J., Leung M. C., Veiseh O., Park J. O., Disis M. L., Zhang M., Chitosan–alginate 3D scaffolds as a mimic of the glioma tumor microenvironment. Biomaterials 31(22), 5903–5910, 2010.

Kim J. H., Park C. H., Perez R. A., Lee H. Y., Jang J. H., Lee H. H., Wall I. B., Shi S., Kim H. W., Advanced biomatrix designs for regenerative therapy of periodontal tissues. Journal of Dental Research 93(12), 1203–1211, 2014.

Kruczkowska W., Kłosiński K. K., Grabowska K. H., Gałęziewska J., Gromek P., Kciuk M., Kałuzińska-Kołat Ż., Kołat D., Wach R. A., Medical applications and cellular mechanisms of action of carboxymethyl chitosan hydrogels. Molecules 29(18), 4360, 2024.

Kumar D., Raj V., Verma A., Kumar P., Pandey J., Novel binary grafted chitosan nanocarrier for sustained release of curcumin. International Journal of Biological Macromolecules 131, 184–191, 2019.

Kumari S., Singh D., Srivastava P., Singh B.N., Mishra A., Generation of graphene oxide and nano-bioglass based scaffold for bone tissue regeneration. Biomedical Materials 17(6), 065012, 2022.

Lam W. A., Chaudhuri O., Crow A., Webster K. D., Li T. D., Kita A., Huang J., Fletcher D. A., Mechanics and contraction dynamics of single platelets and implications for clot stiffening. Nature Materials 10(1), 61–66, 2011.

Larsson L., Decker A. M., Nibali L., Pilipchuk S. P., Berglundh T., Giannobile W. V., Regenerative medicine for periodontal and peri-implant diseases. Journal of Dental Research 95(3), 255–266, 2016.

Li T., Yang J., Liu R., Yi Y., Huang M., Wu Y., Tu H., Zhang L., Efficient fabrication of reversible pH-induced carboxymethyl chitosan nanoparticles for antitumor drug delivery under weakly acidic microenvironment. International Journal of Biological Macromolecules 126, 68–73, 2019.

Lin T., Chen D., Geng Y., Li J., Ou Y., Zeng Z., Yin C., Qian X., Qiu X., Li G., Zhang Y., Guan W., Li M., Cai X., Wu J., Chen W. H., Guan Y. Q., Yao, H., Carboxymethyl Chitosan/Sodium Alginate/Chitosan Quaternary Ammonium Salt Composite Hydrogel Supported 3J for the Treatment of Oral Ulcer. Gels 9(8), 659-, 2023.

Maksoud F. J., Velázquez de la Paz M. F., Hann A. J., Thanarak J., Reilly G. C., Claeyssens F., Green N. H., Zhang Y. S. Porous biomaterials for tissue engineering: a review. Journal of Materials Chemistry B 10(40), 8111–8165, 2022.

Marsh P. D., Do T., Beighton D., Devine D. A., Influence of saliva on the oral microbiota. Periodontology 2000, 70(1), 80–92, 2016.

Meyle J., Chapple I., Molecular aspects of the pathogenesis of periodontitis. Periodontology 2000 69(1), 7–17, 2015.

Pooresmaeil M., Namazi H., Developments on carboxymethyl starch-based smart systems as promising drug carriers: A review. Carbohydrate Polymers 258, 117654, 2021.

Reddi B. A. Why Is Saline So Acidic (and Does It Really Matter?). International Journal of Medical Sciences 10(6), 747–750, 2013.

Reynolds I., Duane B., Periodontal disease has an impact on patients' quality of life. Evidence-Based Dentistry 19(1), 14–15, 2018.

Ryu J. H., Choi J. S., Park E., Eom M. R., Jo S., Lee M. S., Kwon S. K., Lee H., Chitosan oral patches inspired by mussel adhesion. Journal of Controlled Release 317, 57–66, 2020.

Sanz M., European workshop in periodontal health and cardiovascular disease. European Heart Journal Supplements, 12(Suppl B), B2–B2, 2010.

Schwarz F., Derks J., Monje A., Wang H., Peri-implantitis. Journal of Clinical Periodontology 45(S20), 2018.

Shariatinia Z., Carboxymethyl chitosan: Properties and biomedical applications. International Journal of Biological Macromolecules 120, 1406–1419, 2018.

Sindhusha V. B., Doraiswamy, J. N. Evaluating the Biological Properties of Chitosan and Gelatin-Based Scaffold in Saliva and Blood: An In Vitro Study. Cureus 15(11), 2023.

Sivashankari P.R., Prabaharan M., Three-dimensional porous scaffolds based on agarose/chitosan/graphene oxide composite for tissue engineering. International Journal of Biological Macromolecules 146, 222–231, 2020.

Spinks G. M., Lee C. K., Wallace G. G., Kim S. I., Kim S. J., Swelling behavior of chitosan hydrogels in ionic liquid−water binary systems. Langmuir 22(22), 9375–9379, 2006.

Tutwiler V., Litvinov R. I., Lozhkin A. P., Peshkova A. D., Lebedeva T., Ataullakhanov F. I., Spiller K. L., Cines D. B., Weisel J. W., Kinetics and mechanics of clot contraction are governed by the molecular and cellular composition of the blood. Blood 127(1), 149–159, 2016.

Unnithan A. R., Park C. H., Kim C. S., Nanoengineered bioactive 3D composite scaffold: A unique combination of graphene oxide and nanotopography for tissue engineering applications. Composites Part B: Engineering 90, 503–511, 2016.

Van der Schueren L., Steyaert I., De Schoenmaker B., De Clerck K., Polycaprolactone/chitosan blend nanofibres electrospun from an acetic acid/formic acid solvent system. Carbohydrate Polymers 88(4), 1221–1226, 2012.

Venkatesan J., Kim S. K., Nano-hydroxyapatite composite biomaterials for bone tissue engineering—A review. Journal of Biomedical Nanotechnology 10(10), 3124–3140, 2014.

Weber M., Steinle H., Golombek S., Hann L., Schlensak C., Wendel H.P., Avci-Adali M., Blood-contacting biomaterials: In vitro evaluation of the hemocompatibility. Frontiers in Bioengineering and Biotechnology 99(6), 2018.

Yu Y. M., Lu Y. P., Zhang T., Zheng Y. F., Liu Y. S., Xia D. D., Biomaterials science and surface engineering strategies for dental peri-implantitis management. Military Medical Research 11(1), 29, 2024.

Zhang Y., Li Z., Guo H., Wang Q., Guo B., Jiang X., Liu Y., Cui S., Wu Z., Yu M., Zhu L., Chen L., Du N., Luo D., Lin Y., Di P., Liu Y., A biomimetic multifunctional scaffold for infectious vertical bone augmentation. Advanced Science 11(26), 2024.

Zhao Y., Fan T., Chen J., Su J., Zhi X., Pan P., Zou L., Zhang Q., Magnetic bioinspired micro/nanostructured composite scaffold for bone regeneration. Colloids and Surfaces B: Biointerfaces 174, 70–79, 2019.